

Energy spectrum and galvanomagnetic phenomena in the p -type gapless semiconductor HgCdTe under uniaxial compression

A. B. Germanenko, G. M. Min'kov, E. L. Rumyantsev, and O. E. Rut

A. M. Gor'ki Ural State University

(Submitted 16 July 1987)

Zh. Eksp. Teor. Fiz. **94**, 242–254 (August 1988)

We have investigated the Hall constant and longitudinal and transverse magnetoresistances as a function of the uniaxial compression χ and magnetic field H for the p -type gapless semiconductor HgCdTe. We observed several distinctive features in these functional dependences, the most important of which are connected with a radical reshaping of the energy spectrum of free and localized states under compression: formation of a forbidden gap, which grows at a rate of 3.8 meV/kbar, changes in the function $\varepsilon(k_{\perp}, k_{\parallel})$ near the band edge, and an increase in the ionization energy of acceptors at a rate of ~ 1 meV/kbar. For this system, quantization in a magnetic field proceeds in an unusual fashion, a fact which is apparent from the behavior of the Shubnikov-deHaas oscillations and from the nonmonotonic dependence of the forbidden gap width on H : the gap first decreases, vanishing at some field which is strongly dependent on the orientation of \mathbf{H} relative to χ , and then increases. We show that the essential features of our observations concerning the behavior of the galvanomagnetic effect can be explained by using a modified Kane model which takes the uniaxial strain into account.

Past work has shown^{1–3} that uniaxial strain gives rise to a considerable reconstruction of the spectrum of the degenerate valence band Γ_8 and of shallow acceptor states in diamond-structure semiconductors with $\varepsilon_g > 0$. In gapless semiconductors such as HgCdTe, which have an inverted band structure,⁴ the valence band and the conduction band are degenerate at the point $\mathbf{k} = 0$, and both belong to the Γ_8 representation. Uniaxial strain, which lowers the symmetry, will lead under these circumstances to splitting of the valence band and the conduction band. In practice this implies that a new conduction band forms, with its own spectrum of free and localized states. Results of experimental investigations of galvanomagnetic effects in uniaxially deformed gapless semiconductors are available only in a few cases, e.g., Refs. 5, 6, which are incomplete and contradictory.

1. EXPERIMENTAL METHODS

In this paper we present the results of experimental investigations of the Hall coefficient R and the longitudinal (ρ_{\parallel}) and transverse (ρ_{\perp}) magnetoresistances in magnetic fields up to 40 kOe, and in the temperature range 1.8 to 70 K, for uniaxial stresses χ up to 3 kbar; this range of stresses corresponds to the region of elastic deformation. We investigated single-crystal samples of p -HgCdTe with $\varepsilon_g = -(80-40)$ meV and $N_A - N_D$ between 10^{15} and 10^{17} cm⁻³ (N_A, N_D are the acceptor and donor concentrations; see the table). Our determination of the parameter $\varepsilon_g = \varepsilon(\Gamma_6) - \varepsilon(\Gamma_8)$ is based on the magnitude of the effective mass m_n at the bottom of the conduction band which is measured by the method of tunneling spectroscopy in a

quantizing magnetic field⁷; $N_A - N_D$ is determined by finding the value of R in a magnetic field of 250 kOe at the impurity depletion temperature.⁸ Typical sample dimensions were $0.7 \times 0.7 \times 6$ mm³; the uniaxial strain is applied along the sample. Unfortunately, we were not able to cut the samples along the symmetric crystallographic directions; however, it will be clear from subsequent discussions that this is important only in determining the value of the deformation potential constant, which is not the intent of this paper. Measurements were carried out for two orientations of the magnetic field: $\mathbf{H} \parallel \chi \parallel \mathbf{j}$ and $\mathbf{H} \perp \chi \parallel \mathbf{j}$ (\mathbf{j} is the current). Immediately before the measurements, the samples were etched in a 5% solution of bromine in butanol.

2. ENERGY SPECTRUM OF A GAPLESS SEMICONDUCTOR UNDER UNIAXIAL STRAIN

The experimentally-observed functions $\rho(\chi, H, T)$ and $R(\chi, H, T)$ have essentially analogous forms for all samples investigated. As is clear from Figs. 1–3, uniaxial deformation radically changes the behavior of all the galvanomagnetic effects; the conductivity for $H = 0$ decreases by three orders of magnitude as χ increases to 2 kbar; the electron concentration, which equals $(eR_0)^{-1}$, decreases, vanishing at $\chi \approx 1.8$ kbar; the position of the Shubnikov-deHaas oscillations observed for $\chi < 1.2$ kbar changes considerably under higher stresses, and in essentially different ways for $\mathbf{H} \parallel \chi$ and $\mathbf{H} \perp \chi$. A sharp minimum is observed in the longitudinal magnetoresistance for stresses $\chi \geq 1$ kbar in magnetic fields of 5–10 kOe; in this case the value of ρ_{\parallel} decreases 1–3 orders of magnitude. It is clear that these strong modifications of the

TABLE I. Parameters of the samples investigated in this paper.

Sample number	ε_g , meV	$N_A - N_D$, cm ⁻³	$n = (eR_0)^{-1}$, cm ⁻³ $T = 4.2$ K	$R_0\sigma_0$, cm ² /V·sec, $T = 4.2$ K
1	-40	$1 \cdot 10^{15}$	$3.4 \cdot 10^{14}$	$3.5 \cdot 10^6$
2	-40	$1 \cdot 10^{16}$	$3.4 \cdot 10^{14}$	$1.0 \cdot 10^6$
3	-40	$4 \cdot 10^{16}$	$< 6 \cdot 10^{14}$	$> 1.5 \cdot 10^5$
4	-80	$1.5 \cdot 10^{17}$	$1.2 \cdot 10^{15}$	$7.0 \cdot 10^4$

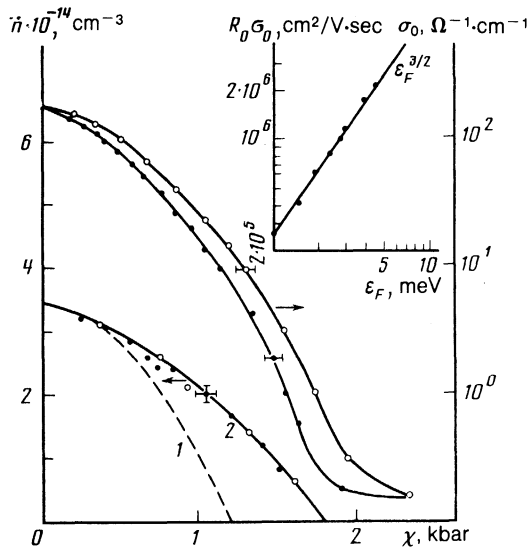


FIG. 1. Electron concentration $n = (eR_0)^{-1}$ and conductivity σ_0 versus the magnitude of the uniaxial stress for sample 1. Curves 1 and 2 are calculations carried out without including the dependence of ϵ_A on χ (1) and including it (2); \bullet —1.8 K, \circ —4.2 K. The inset shows the dependence of the electron mobility $\mu_c = R_0\sigma_0$ on the Fermi energy measured from the bottom of the conduction band.

galvanomagnetic behavior are primarily connected with a reconstruction of the energy spectrum of the unstrained gapless spectrum under uniaxial strain.

Let us investigate in detail the influence of uniaxial strain on the energy spectrum and galvanomagnetic effects for the special case of sample 1, which had the lowest doping level; as we will show below, we were most successful in carrying out a quantitative investigation of the experimental dependences for small values of $N_A - N_D$.

The field and temperature dependences of R, ρ_{\parallel} , and ρ_{\perp} for this sample were investigated in Ref. 9 in the absence of strain; these investigations indicated that the sample was p -type, with a narrow acceptor band whose center was located a distance $\epsilon_A \approx 4.5$ meV from the top of the valence band. In

samples of HgCdTe for which the electron effective mass is small the donors always turn out to be ionized for real donor concentrations; this causes the Fermi level in our sample, as in the majority of pure samples of p -HgCdTe with $\epsilon_g < 0$, to be pinned in the acceptor band,¹⁰ for $H = 0$ and $\chi = 0$ the conductivity and Hall constant in this sample are determined by an electron concentration $(eR_0)^{-1} = 3.4 \times 10^{14}$ cm⁻³ and by a mobility $R_0\sigma_0 \approx 3.5 \cdot 10^6$ cm²/V·sec. In a quantizing magnetic field, the energy of the lowest Landau level of the conduction band equals $\hbar\omega_c/4 \approx \hbar eH/4m_n c$; when this energy becomes larger than the acceptor energy, electrons freeze out onto the acceptor states, which leads to a sharp increase in ρ for $H > 4\epsilon_A m_n c/e\hbar \approx 5.5$ kOe (Fig. 3). Our investigations show that in magnetic fields for which ρ takes on values in excess of 3–5 $\Omega \cdot \text{cm}$, the conductivity of the sample is not determined by its bulk properties, but is apparently related to inclusions of n -type material which form an infinite cluster¹¹; therefore, in what follows we will not discuss any results pertaining to values of H, T, χ for which ρ becomes larger than 1–3 $\Omega \cdot \text{cm}$.

In order to interpret the way that $R, \sigma, R\sigma$ depend on uniaxial strain, it is first of all necessary to know the energy dispersion relations under these conditions. In order to calculate the energy spectrum in this case, it is necessary to augment the $6 \times 6 \mathbf{k} \cdot \mathbf{p}$ Hamiltonian which is used to take into account the interaction between the Γ_6 and Γ_8 bands with new terms which describe the influence of uniaxial deformation [in our case we can neglect the influence of the Γ_7 band, since in HgCdTe we have $\epsilon(\Gamma_8) - \epsilon(\Gamma_7) \gg \epsilon, \epsilon_g$]. In the absence of strain the energy spectrum of HgCdTe is rather well described by the isotropic approximation,⁴ for which the form of the Hamiltonian does not depend on the orientation of \mathbf{H} and χ relative to the crystallographic axes, for $\mathbf{H} \parallel \chi \parallel \mathbf{z}$ the energy dispersion law $\epsilon(k_{\perp}, k_{\parallel})$, where $k_{\perp}^2 = kx^2 + ky^2, k_{\parallel} = kz$, is determined by the solution to the Schrödinger equation with the Hamiltonian

$$\hat{H} = \begin{vmatrix} \hat{H}(\Gamma_6) & \hat{A} \\ \hat{A}^+ & \hat{H}(\Gamma_8) \end{vmatrix}, \quad (1)$$

where

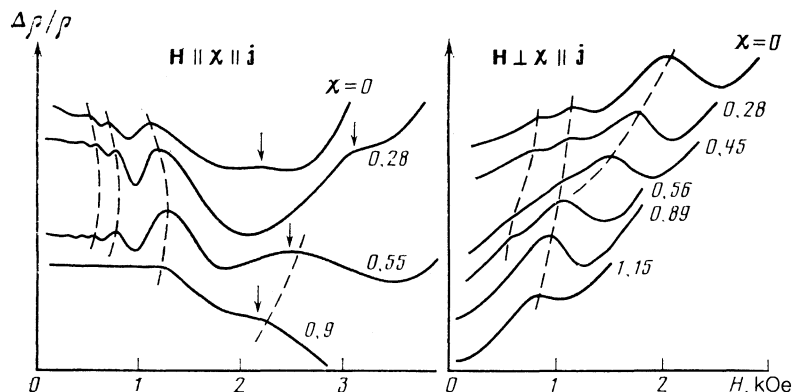


FIG. 2. The oscillatory part of the magnetoresistance for two orientations of the magnetic field relative to the direction of compression for sample 1 at $T = 1.8$ K. We denote by arrows the position of the last maximum of ρ for $\mathbf{H} \parallel \chi$. The numbers next to the curves are pressures in kilobars. The dashed lines show the motion of the oscillation maxima as the pressure varies.

$$\hat{H}(\Gamma_6) = \begin{vmatrix} H_{11}(\Gamma_6) & 0 \\ 0 & H_{22}(\Gamma_6) \end{vmatrix},$$

$$\hat{A} = \begin{vmatrix} -\left(\frac{sE_p}{2}\right)^{1/2} a^+ & \left(\frac{sE_p}{3}\right)^{1/2} Lk_z & \left(\frac{sE_p}{6}\right)^{1/2} a & 0 \\ 0 & -\left(\frac{sE_p}{6}\right)^{1/2} a^+ & \left(\frac{sE_p}{3}\right)^{1/2} Lk_z & \left(\frac{sE_p}{2}\right)^{1/2} a \end{vmatrix},$$

$$\hat{H}(\Gamma_8) = \begin{vmatrix} H_{11}(\Gamma_8) & 6^{1/2}s\bar{\gamma}Lk_za & 3^{1/2}s\bar{\gamma}a^2 & 0 \\ 6^{1/2}s\bar{\gamma}Lk_za^+ & H_{22}(\Gamma_8) & 0 & 3^{1/2}s\bar{\gamma}a^2 \\ 3^{1/2}s\bar{\gamma}(a^+)^2 & 0 & H_{33}(\Gamma_8) & -3^{1/2}s\bar{\gamma}Lk_za \\ 0 & 3^{1/2}s\bar{\gamma}(a^+)^2 & -6^{1/2}s\bar{\gamma}Lk_za^+ & H_{44}(\Gamma_8) \end{vmatrix},$$

$$H_{11}(\Gamma_6) = \varepsilon_g + s(\hat{n}+1) + 1/2sL^2k_z^2 + \delta\varepsilon_g + 5P,$$

$$H_{22}(\Gamma_6) = H_{11}(\Gamma_6) + s,$$

$$H_{11}(\Gamma_8) = -s[(\gamma_1 + \bar{\gamma})(\hat{n} + 1/2) + 3/2k^+ + 1/2(\gamma_1 - 2\bar{\gamma})L^2k_z^2] + 9P,$$

$$H_{44}(\Gamma_8) = -s[(\gamma_1 + \bar{\gamma})(\hat{n} + 1/2) - 3/2k^+ + 1/2(\gamma_1 - 2\bar{\gamma})L^2k_z^2] + 9P,$$

$$H_{22}(\Gamma_0) = -s[(\gamma_1 - \bar{\gamma})(\hat{n} + 1/2 + 1/2k^+ + 1/2(\gamma_1 + 2\bar{\gamma})L^2k_z^2) + P],$$

$$H_{33}(\Gamma_8) = -s[(\gamma_1 - \bar{\gamma})(\hat{n} + 1/2) - 1/2k^+ + 1/2(\gamma_1 + 2\bar{\gamma})L^2k_z^2] + P;$$

$E_p = 2m_0P^2/\hbar^2$ (P is the matrix element of the momentum operator), $\gamma_1 = \gamma_1^L - E_p/3\varepsilon_g$, $\bar{\gamma} = \bar{\gamma}^L - E_p/6\varepsilon_g$, $k = k^L - E_p/6\varepsilon_g$ ($\gamma_1^L, \bar{\gamma}^L, \gamma_2^L = \gamma_3^L, k^L$ are the Luttinger parameters); $L = (c\hbar/eH)^{1/2}$ is the magnetic length; $s = \hbar eH/m_0c$ is the cyclotron energy of a free electron; $a = L(k_x + ik_y)/2^{1/2}$, $a^+ = L(k_x - ik_y)/2^{1/2}$ are creation and annihilation operators. P is a constant describing the splitting of the Γ_8 band under uniaxial strain; generally speaking, P depends on the direction of χ relative to the crystallographic axes. For $\chi \parallel [111]$, $[100]$, P equals $dS_{44}\chi/8 \cdot 3^{1/2}$ and $b(S_{11} - S_{12})\chi/4$, respectively, where b, d are deformation potential constants, and S_{11}, S_{12} , and S_{44} are components of the elastic compliance tensor; $\delta\varepsilon_g$ is the variation of ε_g with strain.

In all our calculations the following parameters were used for HgCdTe: $\gamma_1 = 2$, $\bar{\gamma} = k = 0$; this choice of param-

eters corresponds to a heavy hole mass $m_h = (\gamma_1 - 2\bar{\gamma})^{-1}m_0 = 0.5m_0$, and $E_p = 17$ eV.¹⁰ Additional investigations which we have carried out concerning the effect of uniaxial strain on the intrinsic electron concentration in n -HgCdTe with $\varepsilon_g(4.2 \text{ K}) = 15$ meV, $N_D - N_A = 10^{14} \text{ cm}^{-3}$ show that the value of $\delta\varepsilon_g/\delta\chi$ is less than 4 meV/kbar, so that in what follows we will not include it. Therefore, in the approximation we are using the effect of uniaxial strain on the energy spectrum of HgCdTe is described by only one constant P .

In Fig. 4 we show the way the spectrum $\varepsilon(k_\perp, k_\parallel)$ changes under uniaxial strain, along with cross sections of the isoenergetic surfaces obtained from (1) in the energy range of interest. In the absence of strain, the degenerate conduction and valence bands are split by an amount $8|P|$ at $\mathbf{k} = 0$; the dependence of the valence band energy on k_\perp becomes nonmonotonic, and the conduction band becomes anisotropic near its bottom, with $m_\parallel \approx 3\varepsilon_g m_0/2E_p = m_i$ and $m_\perp = 6\varepsilon_g m_0/E_p = 4m_i$ (m_i is the light-hole mass). The forbidden gap Δ which appears under strain is smaller than the splitting at $\mathbf{k} = 0$; for $m_h = 0.5m_0$, Δ is roughly equal to $2.5|P|$. As is clear from Fig. 4b, the isoenergetic surfaces of the valence band for small energies are tori, which degenerate into deformed ellipsoids as the energy increases.

In order to understand how the galvanomagnetic effects in p -type gapless semiconductors depend on the magnitude of the uniaxial compression, it is necessary to know not only the spectrum of the carrier bands but also the position of the acceptor level. Since uniaxial strain leads to the appearance of a forbidden gap which increases with increasing χ , the shallow acceptor level which splits off from the top of the valence band must sink below the bottom of the conduction band (Fig. 4a) at a certain value of χ . Therefore, in gapless p -type semiconductors for which the conductivity is determined by electrons at $\chi = 0$, uniaxial strain must lead to a decrease in the energy of the Fermi level which is pinned at the acceptor, and thus a fall in the electron concentration and a rise in the specific resistivity. For some value of χ the acceptor level emerges into the forbidden band; when this happens, the electron concentration at low temperatures must become exponentially small.

For a quantitative description of the observed dependences, it is necessary to know the constant P which describes the splitting of the bands under compression; when this is known, the splitting can be computed for any orientation of χ . However, reliable data on the deformation potential constant cannot be found in the literature. Therefore, we determined the value of P experimentally by comparing the measured temperature dependence of the electron concen-

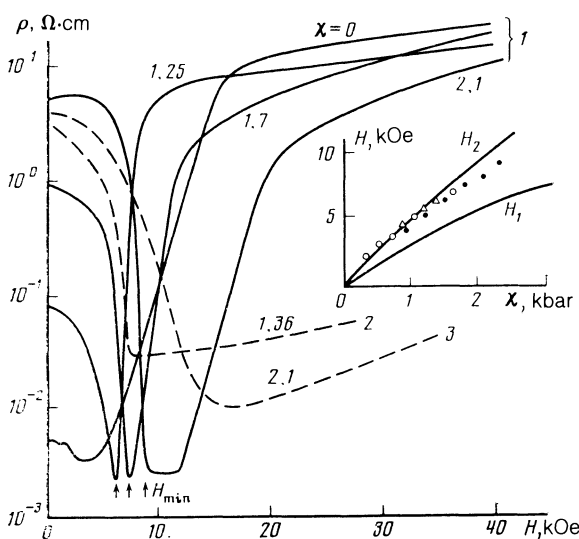


FIG. 3. Longitudinal magnetoresistance of the samples under study for the orientation $\mathbf{H} \parallel \chi$ at $T = 4.2 \text{ K}$; 1—sample 1; 2—sample 2; 3—sample 3. The numbers on the curves are pressures in kilobars. In the inset we show the experimental dependence of H_{\min} on pressure for sample 1 (\bullet), 2 (\circ), 3 (Δ) and the theoretical functions $H_1(\chi)$ and $H_2(\chi)$.

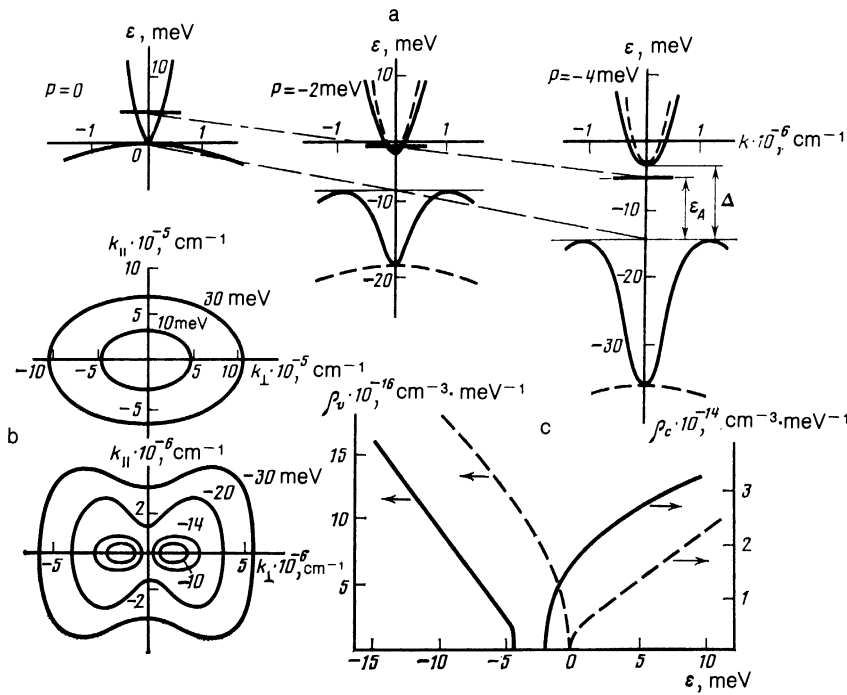


FIG. 4. (a) Reshaping of the energy spectrum of a HgCdTe-type gapless semiconductor under uniaxial strain. The continuous curves are the functions $\varepsilon(k_{\perp})$ for $k_{\parallel} = 0$; the dashed curves are $\varepsilon(k_{\parallel})$ for $k_{\perp} = 0$; (b) the isoenergetic surfaces near the bottom of the conduction band (the upper curves) and near the top of the valence band (lower curves) for $P = -2$ meV. The numbers on the curves are energies in meV; (c) the density of states near the band extrema in the absence of deformation (dashed curves) and under uniaxial strain (continuous curves), $P = -2$ meV.

tration for various values of the compression with the concentration calculated from the charge neutrality equation (Fig. 5);

$$n + N_{A^{-}} = N_{D^{+}} + p,$$

$$n = \int \rho_c(\varepsilon) f(\varepsilon, \varepsilon_F) d\varepsilon, \quad p = \int \rho_v(\varepsilon) f(\varepsilon, \varepsilon_F) d\varepsilon,$$

$$N_{A^{-}} = N_A f(\varepsilon_A, \varepsilon_F), \quad \rho_{c,v} = \frac{1}{\pi^2} \int dk_{\perp} k_{\perp} \frac{\partial k_{\parallel}}{\partial \varepsilon}. \quad (2)$$

The dependence of $\partial k_{\parallel} / \partial \varepsilon$ on k_{\perp} , ε in the expressions for the density of states in the valence and conduction bands should be taken from the solution to Eq. (1).

As our numerical calculations show, the densities of states in the valence and conduction bands change considerably under uniaxial strain (Fig. 4c). Analysis of the temperature dependence of the electron concentration computed from the charge neutrality condition (2) including the variation of $\varepsilon_g(T)$ (Ref. 11) shows that for temperatures above 15–20 K and $N_A - N_D \approx 10^{15}$ cm $^{-3}$ the source of most of the electrons is thermal excitation from the valence band rather than from the acceptors; therefore at these temperatures $n(T)$ is determined by only one parameter P . Thus, by comparing the theoretical and experimental functions $n(T)$ for various χ (Fig. 5) we obtain the value $P = -(1.5 \pm 0.08)$ [meV/kbar] χ .

At temperatures below 15 K the electron concentration is determined to a considerable extent by the position of the acceptor level. It is clear from Fig. 5 that there are significant discrepancies between the experimental and theoretical functions $n(T)$ at low temperatures if it is assumed that the ionization energy of an acceptor (i.e., its energy measured from the top of the valence band) does not depend on χ . Good agreement is achieved if it is assumed that ε_A increases linearly with increasing compression; specifically, $\varepsilon_A(\chi) = \varepsilon_A(0) + 1$ [meV/kbar] χ (Fig. 5). The electron concentration at $T = 1.8$ K calculated using this dependence on the magnitude of the strain gives a good description of the

experimental function $n(\chi)$ (see Fig. 1). For comparison, on the same figure we show the function $n(\chi)$ calculated by assuming that $\varepsilon_A = \text{const} = 4.5$ meV.

One possible reason for the increase in the acceptor ionization energy under uniaxial strain could be the variation of the dielectric permittivity κ . Actually, in a gapless semiconductor with $\chi = 0$ electron-electron interactions do in fact give rise to a correction $\Delta\kappa = 8me^2/\pi\hbar^2 k_F$ (Ref. 4), which

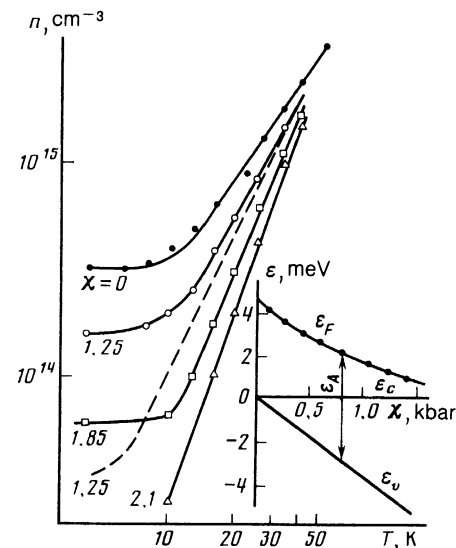


FIG. 5. Temperature dependence of the electron concentration. The points are experiment (sample 1); the dashed curves are theoretical functions obtained by assuming that ε_A does not depend on pressure and equals 4.5 meV; the continuous curves are these functions with $\varepsilon_A(\chi) = 4.5$ meV + 1 [meV/kbar] χ . In the calculations we set $P = -1.5$ [meV/kbar] χ . The numbers on the curves are pressures in kilobars. In the inset we show the pressure dependence of the Fermi level measured from the bottom of the conduction band. We also show here the position of the top of the valence band for $T = 1.8$ K.

decreases as the width of the compression-induced forbidden gap increases. In addition to this, uniaxial strain significantly changes the valence band spectrum $\varepsilon_v(k_\perp, k_\parallel)$; however, we know of no paper in which the energy is calculated for an impurity state split off from a valence band whose isoenergetic surfaces are in the shape of tori.

Uniaxial strain leads to a decrease in the conductivity which is considerably more rapid than that of the carrier concentration (Fig. 1), indicating a decrease in electron mobility $\mu_e = R_0 \sigma_0$. For a degenerate gas of electrons undergoing scattering by ionized impurities we have $\mu \approx e\tau/m^* \sim \varepsilon_F^{3/2}(\chi)/m^*$. In our case the conductivity is measured along the direction of compression; therefore the conductivity is determined by the longitudinal effective mass $m^* = m_\parallel$, which, as follows from (1), is independent of χ and is roughly equal to m_n . Therefore, the decrease in μ_e with compression is determined by the variation of $\varepsilon_F(\chi)$. The position of the Fermi level relative to the bottom of the conduction band can be directly determined from the electron concentration at $T = 1.8$ K (when the electron gas is degenerate) and the density of states calculated using the value of P determined above (Fig. 5). It is clear from the inset in Fig. 1 that the exponent in the dependence of μ_e on ε_F is in fact close to $3/2$.

Thus, analysis of the functions $n(\chi, T)$ and $\sigma(\chi, T)$ shows that uniaxial strain gives rise to splitting of the conduction band and valence band at $k = 0$ by an amount $8|P| = 8 \cdot (1.5 \pm 0.2)$ [meV/kbar] χ and the formation of a forbidden gap $\Delta \approx 2.5|P| \approx 3.8$ [meV/kbar] χ . In this case the acceptor energy measured from the top of the valence band, which is shifted from the point $k = 0$, increases; $\varepsilon_A(\chi) = \varepsilon_A(0) + 1$ [meV/kbar] χ , and at a pressure of $\chi = 1.8$ kbar the acceptor emerges into the forbidden gap. The decrease of ε_F with increasing χ also leads to a drop in the electron mobility.

3. SHUBNIKOV-DEHAAS OSCILLATIONS UNDER UNIAXIAL STRAIN

For small strains, as long as the acceptor level is located in the background of conduction band states and the electron gas is degenerate, we can observe Shubnikov-deHaas oscillations in magnetic fields $H < 3$ kOe (Fig. 2). The position of these oscillations in a magnetic field is determined by the condition of $\varepsilon_F(\chi) = \varepsilon_n(\chi, H)$ (ε_n is the n th Landau level

energy at $k = 0$). As we described earlier, the Fermi level in the samples we studied is pinned at the acceptor level, whose energy, just as that of the Landau level energy, depends on the magnitude of the compression; therefore, the position of the Shubnikov-deHaas oscillations should depend on χ . The experimental dependence of the positions of the maxima of the magnetoresistance on the magnitude of the uniaxial compression for two magnetic field orientations, $\mathbf{H} \parallel \chi \parallel \mathbf{j}$ and $\mathbf{H} \perp \chi \parallel \mathbf{j}$, is shown in Fig. 6.

The theoretical position of the Fermi level for $\chi \parallel \mathbf{H}$ can be obtained from the solution of the Schroedinger equation with the Hamiltonian (1) by selecting wave functions whose form is analogous to that of the wave functions for $\chi = 0$, since for $\chi \parallel \mathbf{H}$ the strain does not further lower the symmetry.

However, in the $\mathbf{H} \perp \chi$ orientation, uniaxial strain lowers the symmetry; therefore the structure of the Hamiltonian is not as simple as (1) (see Ref. 1), and it is not possible to obtain an exact solution in the general case. In this situation, we have chosen to solve the problem approximately; the wave function is sought in the form of an expansion in solutions to the unperturbed problem (i.e., for $\chi = 0$). Taking into account the interactions of the N nearest Landau levels reduces the problem to evaluating a $6N$ -order determinant. We have analyzed the numerical solution and compared it with an exact solution which is available when $m_h^{-1} = (\gamma_1 - 2\bar{\gamma})m_0^{-1} = 0$, and have found that by taking into account eight levels we obtain an accuracy of 0.1 meV or better in determining the energy of the lowest five conduction-band Landau levels, and 0.2 meV or better for the top-most Landau level energy of the valence band. Theoretical calculations of the Landau level energies at $k_x = 0$ in both orientations of magnetic field relative to the direction of compression are given in the insets of Fig. 6.

Using the position of the Fermi level determined in the previous section (which coincides with the acceptor level at low temperatures; see the inset in Fig. 5) along with the computed functions $\varepsilon_n(H)$, and assuming that ε_A does not depend on H in the region of low magnetic fields,²⁾ we can compare the theoretically calculated positions of the Shubnikov-deHaas oscillation maxima with the experimental results (Fig. 6). It is clear that the behavior of the oscillations as χ varies differs for the two magnetic field orientations relative to the direction of compression. The essential fea-

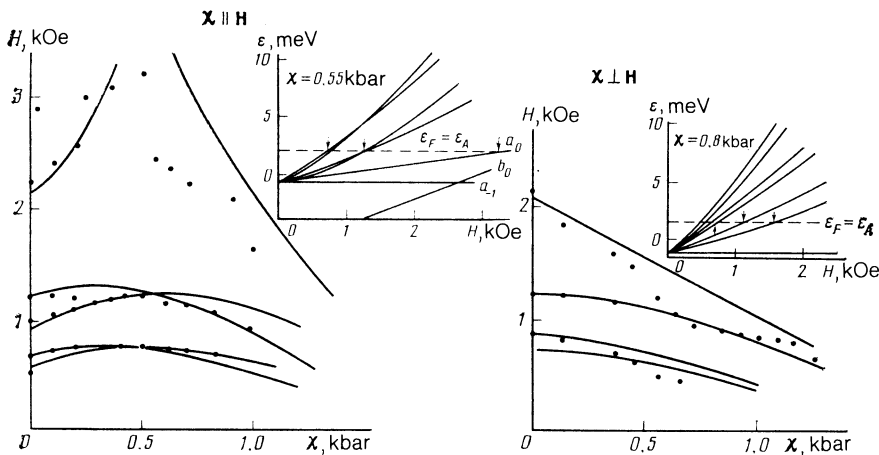


FIG. 6. Dependence of the positions of the maxima of the Shubnikov-deHaas oscillations in sample 1 for $T = 1.8$ K on the magnitude of the uniaxial compression for two orientations of the \mathbf{H} relative to χ . In the inset we show the position of the Landau level calculated from (1) and the experimentally determined position of the Fermi level.

tures of our experimental results agree rather well with the theory based on the model under study here. The singularity in the position of the uppermost maximum in $\rho_{\parallel}(H)$ at $\chi \approx 0.5$ kbar is connected with the fact that this maximum is determined by the intersection of ε_F with the level b_0 for small χ , and with the level a_0 for large χ (Figs. 6, 7).

4. MAGNETORESISTANCE OF A UNIAXIALLY DEFORMED GAPLESS p -TYPE SEMICONDUCTOR

So as to explain the behavior of the longitudinal magnetoresistance in p -type HgCdTe under uniaxial strain, we now investigate the variation of the width of the forbidden band Δ in a magnetic field. It is clear from Fig. 7 that in the region of small magnetic fields Δ depends weakly on H up to a field $H = H_1$, at which the level b_0 is no longer the topmost Landau level of the valence band. For $H > H_1$ the width Δ rapidly decreases, vanishing at $H = H_2$. In this field the Landau level b_0 intersects the level a_{-1} ; these two levels change the sign of the curvature (i.e., the sign of $\partial^2 \varepsilon / \partial k_z^2$ for $k_z \approx 0$), so that for $H > H_2$ the forbidden band appears again; for $H_2 < H < H_3$ it is determined by the spacing between the levels a_{-1} and b_0 , for $H > H_3$ by the spacing between a_{-1} and a_0 . It is clear that if we start with a strain that puts the Fermi level in the forbidden band at $H = 0$ (Figs. 4, 7), the Fermi level will necessarily be found in the region of the continuous spectrum as the magnetic field increases to $H \approx H_2$; this gives rise to the appearance of free carriers and to a sharp decrease in ρ_{\parallel} . The value of the field H_2 can be obtained from the Hamiltonian (1) when we set the energies of levels a_{-1} and b_0 equal:

$$\begin{aligned} \varepsilon_{a_{-1}} &= -s^{1/2}(\gamma_1 - \bar{\gamma}) - 1/2 k^2 + P, \\ \varepsilon_{b_0} &= 1/2 [\varepsilon_g - 3/2 s(\gamma_1 + \bar{\gamma} - k) + 9P] \\ &+ 1/2 \{ [\varepsilon_g - 3/2 s(\gamma_1 + \bar{\gamma} - k) + 9P]^2 + 2sE_p \}^{1/2}. \end{aligned} \quad (3)$$

In the parabolic approximation the expression for H_2 has a simple form:

$$H_2 = \frac{8P}{\gamma_1^L + 2\bar{\gamma}^L - k^L} \frac{m_0 c}{e \hbar}. \quad (4)$$

It is clear from (4) that H_2 is shifted to the side of large fields as χ increases. We present in the inset of Fig. 3 the experimental dependences $H_{\min}(\chi)$ and $H_2(\chi)$ calculated from (3). In the same figure, we show the dependence of the mag-

netic field $H_1(\chi)$ obtained from (1), i.e., the field for which the topmost Landau level of the valence band becomes the level b_0 (see Fig. 7a). As is clear from Fig. 3, the experimental values of H_{\min} lie between H_1 and H_2 .

So as to elucidate what sort of carriers determine the conductivity in a magnetic field $\mathbf{H} \parallel \chi \parallel \mathbf{j}$ equal to H_{\min} , we measured the Hall coefficient, whose sign corresponds to holes. (In order to measure R for $\mathbf{H} \parallel \chi$ we applied an additional transverse magnetic field whose strength was 500 Oe). If we assume that for $H = H_{\min}$ all acceptors are ionized and that $p = N_A - N_D = 10^{15} \text{ cm}^{-3}$, then an estimate of the value of the hole mobility gives $\mu = \sigma / ep \approx 10^6 \text{ cm}^2/\text{V}\cdot\text{sec}$, which agrees with the small effective mass at the top of the uppermost Landau level of the valence band for $H = H_{\min}$.

In order to discuss the function $\rho_{\parallel}(\chi, H)$ in more detail it is necessary to know the behavior of the acceptor states in a magnetic field. As is clear from Fig. 7a, for $H > H_1$ the ground state of the impurity center can be split off both from the uppermost valence band (b_0 for $H < H_2$ or a_1 for $H > H_2$) and from the group of closely-spaced levels of the valence band.

If the state which splits off from the group of closely-spaced Landau levels is the ground state of the acceptor, then the observed behavior of $\rho_{\parallel}(\chi, H)$ can be explained if we assume that in magnetic fields close to H_2 this state is a resonance and lies in the background of valence band states (i.e., the levels b_0 and a_{-1}) (Fig. 7a).

In the other case, when the ground state of the acceptor is a state split off from one of the Landau levels, the magnetic field can produce an insulator-metal transition for $H < H_2$ and a metal-insulator transition for $H > H_2$. Actually, in those magnetic fields for which the spacing between the uppermost Landau level and the following level exceeds the ionization energy $\varepsilon_A(H)$, the size of the wave function of the localized state in a direction perpendicular to H is determined by the magnetic length $a_{\perp} = L = (c\hbar/eH)^{1/2}$, while in directions perpendicular to H it is determined by the quantity $a_{\parallel} \approx \hbar^2 [2m_{\parallel} \varepsilon_A(H)]^{-1/2}$. The value of m_{\parallel} near $H = H_2 \approx 10 \text{ kOe}$ is of order $10^{-3} m_0$, which gives for $\varepsilon_A(H) = 1 \text{ meV}$ the values $a_{\perp} \approx 8 \cdot 10^{-6} \text{ cm}$, $a_{\parallel} \approx 10^{-5} \text{ cm}$. In this case, at impurity concentrations $N > 3 \cdot 10^{13} \text{ cm}^{-3}$ the product $Na_{\perp}^2 a_{\parallel}$ will be larger than the value 0.02 which corresponds to the Mott transition, so that the localized states at the impurities disappear while the concentration of free holes becomes equal to $N_A - N_D$.

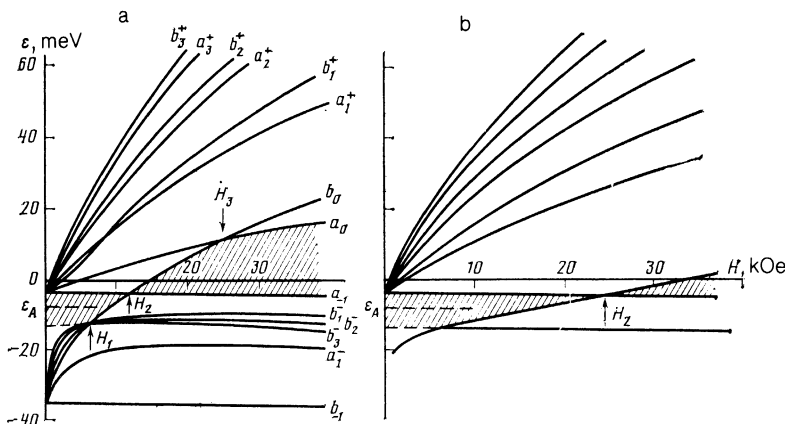


FIG. 7. Position of the Landau levels for $\mathbf{H} \parallel \chi$ (a) and $\mathbf{H} \perp \chi$ (b) in the uniaxially strained gapless semiconductor HgCdTe with parameters corresponding to sample 1 for $\chi = 2.6$ kbar. The crosshatched region is the forbidden band. Classification of the Landau level for $\chi \parallel \mathbf{H}$ corresponds to the Pidgeon-Brown classification. In the $\chi \perp \mathbf{H}$ case the eigenfunctions are complicated combinations of the $\chi = 0$ Landau level wave functions; therefore, it is not permissible to carry out the same type of classification as for $\mathbf{H} \parallel \chi$.

In magnetic fields $H > H_2$, when the forbidden gap opens up again, the growth in the value of m_{\parallel} at the top of the uppermost Landau level and the decrease in the magnetic length result in a compression of the acceptor wave function; this ensures that $NL^2 a_{\parallel}$ will become smaller than 0.02, so that the acceptor states are split off and magnetic freeze-out of the holes takes place. These effects also lead to a strong increase in ρ for $H > H_2$.

A sharp decrease in resistivity for $H = 5-10$ kOe is observed in all the samples we investigated; however, in more heavily doped samples with $N_A - N_D > 4 \cdot 10^{16} \text{ cm}^{-3}$ there is no growth in $\rho(H)$ above 50 kOe (Fig. 3). This behavior of ρ can be explained using either model of the impurity states; for the first model (when the ground state of the acceptor is split off from the group of closely-spaced large- m_{\parallel} Landau levels, Fig. 7a) this behavior is connected with the fact that an increase in impurity concentration leads to a decrease in the ionization energy of the acceptor, so that its level remains a resonance for all values of magnetic field. In the second model, the absence of growth in ρ in large magnetic fields can be explained by the fact that in these samples $Na_1^2 a_{\parallel}$ always remains larger than 0.02. As we see it, the available experimental data and theoretical calculations do not allow us to determine which of the two acceptor states described above is the ground state in a magnetic field.

The dependence of the width of the forbidden band on magnetic field in a uniaxially strained semiconductor should be nonmonotonic, as is clear from Fig. 7. As we showed above, the width of the forbidden band which opens up under uniaxial strain in the absence of a magnetic field can be reliably determined by using the temperature dependence of the Hall coefficient, since $R = (ne)^{-1}$. We were not able to measure the temperature dependence of the electron concentration in a strong magnetic field for the orientation $\mathbf{H} \parallel \chi \parallel \mathbf{j}$. In this case the width of the forbidden band can be estimated from the temperature dependence of $\rho(T)$ given in Fig. 8. It is clear from the inset of Fig. 8 that for $H = 0$ the value of the activation energy of the conductivity determined from the slope of the temperature dependence of $\lg \rho_{\parallel}$ versus $1/T$ for $T > 20$ K differs somewhat for the value of Δ obtained from

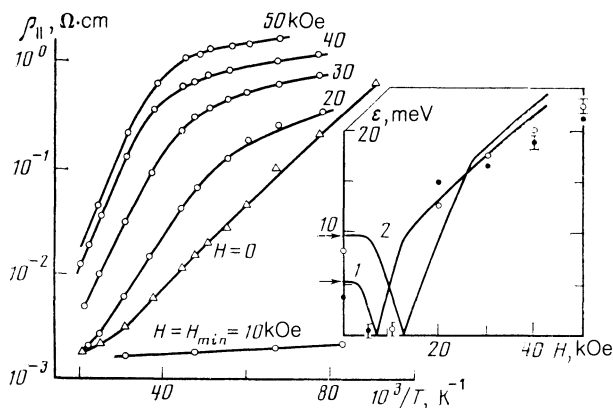


FIG. 8. Temperature dependence of the specific resistivity of sample 1 subjected to uniaxial pressure in various magnetic fields $\mathbf{H} \parallel \chi \parallel \mathbf{j}$ for $\chi = 2.34$ kbar. In the inset, the points are activation energies obtained from experimental dependences of $\lg \rho$ on $1/T$ for two values of χ (\bullet —1.25 kbar, \circ —2.34 kbar); the arrows denote values obtained from the temperature dependence of the electron concentration; the continuous curves 1 and 2 are the theoretical dependences of the forbidden band widths on magnetic fields for $\chi = 1.25$ and $\chi = 2.34$ kbar, respectively.

an analysis of the temperature dependence of the electron concentration; this is connected with our ignoring the temperature dependence of $\mu(T)$ and the effective numbers of band states $N_c(T)$ and $N_v(T)$. Therefore the value of the activation energy for the conductivity Δ_{σ} should only qualitatively reflect the behavior of the forbidden band even in a magnetic field. The function $\Delta_{\sigma}(H)$ shown in Fig. 8 reveals that Δ_{σ} vanishes for $H = H_{\min}$; however, it increases rapidly as the magnetic field increases. On the same figure we show the theoretical function $\Delta(H)$ (the crosshatched region in Fig. 7); it appears that $\Delta(H)$ agrees rather well with the behavior of the activation energy of the conductivity. It must be kept in mind that for $H > H_3$ the width of the forbidden band is determined by the spacing between the levels a_{-1} and a_0 (Fig. 7a) which, as our analysis shows, depends weakly on the magnitude of the compression.

In contrast to the magnetoresistance for the orientation $\mathbf{H} \parallel \chi \parallel \mathbf{j}$ (Fig. 3), we see no deep minimum in the function $\rho_{\perp}(H)$ (i.e., in the orientation $\mathbf{H} \perp \chi \parallel \mathbf{j}$) under uniaxial strain (Fig. 9); this is apparently connected with a large positive transverse magnetoresistance which arises because of the high carrier mobilities ($\mu_e, \mu_h \approx 10^6 \text{ cm}^2/\text{V} \cdot \text{sec}$). In addition, the Landau levels behave in profoundly different ways for the two orientations of magnetic field relative to the direction of compression. As the calculations show, (Fig. 7b), for $\mathbf{H} \perp \chi$ the crossing and inversion of the Landau levels of the valence band and conduction band occur at large magnetic fields. However, even in this orientation we observe a rather small minimum for $\chi > 1.5$ kbar which shifts in the direction of the large magnetic fields as χ increases (Fig. 9). On the same figure we show the dependence of the magnetic field for which the crossing of the Landau levels of the valence and conduction bands leads to the disappearance of the forbidden gap in the orientation $\mathbf{H} \perp \chi$. In this case, too, our calculations describe the experimental dependence rather well.

The essential features of the behavior of R and ρ described above as a function of the magnitude of the uniaxial compression and the magnetic field intensity are observed in all samples we studied. We did not observe the nonmono-

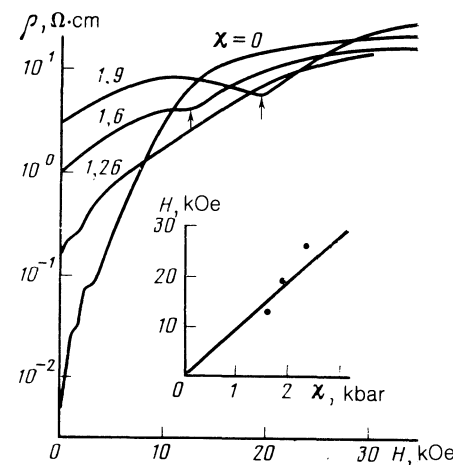


FIG. 9. Dependence of the specific resistivity of sample 1 on magnetic field for $T = 4.2$ K in the orientation $\mathbf{H} \perp \chi \parallel \mathbf{j}$. The numbers on the curves are pressures in kilobars. The inset shows the pressure dependence of the position of the minimum of ρ (the points) and the calculated function $H_2(\chi)$.

tonic dependence $\rho(\chi)$ reported in Ref. 6 (i.e., a strong fall-off in resistance for large compressions) in even one of these samples at $H = 0$. This behavior of $\rho(\chi)$ was interpreted by the authors of Ref. 6 to be a consequence of the decrease in ionization energy of the acceptor and an insulator-metal transition under uniaxial compression, which contradicts the conclusions of this paper concerning the increase of ε_A with increasing χ . From our viewpoint, the results of Ref. 6 can be understood only if we assume that the $\text{Hg}_{1-x}\text{Cd}_x\text{Te}$ samples under investigation, which had compositions $x = 0.155\text{--}0.157$ which were very close to the composition $x = 0.16$ at which the gapless semiconductor to normal semiconductor transition occurs, in actuality contained p -type regions with $\varepsilon_g > 0$ and with $\varepsilon_g < 0$. If each of these regions forms an infinite cluster, then the resistivity of such a sample will be determined by regions with the smallest ρ . For small compressions these are the regions with $\varepsilon_g < 0$ for which ρ increases as χ increases, while for larger compressions they are the regions with $\varepsilon_g > 0$ for which, as was shown in Ref. 12, the resistivity falls abruptly.

CONCLUSION

Our investigations of galvanomagnetic effects in p - HgCdTe with $\varepsilon_g < 0$ under uniaxial strain show that the observed features of the experimental dependences $R(H, \chi, T)$ and $\rho(H, \chi, T)$ are caused by reshaping of the energy spectrum of the gapless semiconductor under the action of the uniaxial strain. This uniaxial strain leads to the formation of a forbidden gap which increases with pressure. In this case a semiconductor with unique properties is created: in the region of small energies the isoenergetic surfaces of the valence band have the form of tori, while those of the conduction band are ellipsoids; quantization of such a spectrum in magnetic field leads first to a decrease in the forbidden gap, which goes to zero at a certain magnetic field H , followed by an increase in this gap. The value of the magnetic field at which the forbidden gap vanishes increases as the pressure increases and depends sensitively on the orientation of χ rel-

ative to H . This feature is well described by a modification of the isotropic Kane model which takes into account uniaxial strain.

Variation of the band spectrum under uniaxial strain also gives rise to a reshaping of the impurity states. We have shown that the acceptor ionization energy increases with uniaxial compression.

¹It was shown in Ref. 9 that for sample 2 the effect of shunting mechanisms does not manifest itself up to values of $\rho \approx 10^4 \Omega \cdot \text{cm}$. Unfortunately, a detailed investigation of this sample under uniaxial strain could not be carried out.

²In magnetic fields $H < H_1$ (Fig. 7) the spacing between Landau levels of the valence band is much less than the acceptor ionization energy; therefore the effect of quantization of the spectrum on ε_A in these fields can apparently be neglected.

³G. L. Bir and G. E. Pikus, *Simmetriya i Deformatsionnye Effekty v Poluprovodnikakh* (Symmetry and Strain Effects in Semiconductors), Moscow: Nauka, 1972.

⁴J. A. Chrobczek, F. N. Pollak, and H. F. Staunton, *Phil. Mag.* **B50**, 113 (1984).

⁵A. V. Germanenko, G. M. Min'kov, and O. E. Rut, *Fiz. Tverd. Tela* (Leningrad) **21**, 2006 (1984) [*Sov. Phys. Solid State* **21**, 1252 (1984)].

⁶I. M. Tsidil'kovskii *Band Structure of Semiconductors*, Pergamon, Oxford (1982).

⁷K. Takita, K. Onabe, and S. Tanaka, *Phys. Stat. Solidi* (b)**92**, 297 (1979).

⁸F. T. Vas'ko, S. G. Gasan-zade, V. A. Romanka, and G. A. Shepel'skii, *Pis'ma Zh. Eksp. Teor. Fiz.* **41**, 100 (1985) [*JETP Lett.* **41**, 120 (1985)].

⁹L. P. Zverev, V. V. Kruzhaev, G. M. Min'kov, and O. E. Rut, *Zh. Eksp. Teor. Fiz.* **80**, 1163 (1981) [*Sov. Phys. JETP* **53**, 595 (1981)].

¹⁰C. T. Eliot, J. Melngailis, T. C. Harman *et al.*, *Phys. Rev.* **B5**, 2985 (1972).

¹¹A. V. Germanenko, V. V. Kruzhaev, G. M. Min'kov, and O. E. Rut, *Fiz. Tekh. Poluprovod.* **22**, 992 (1988) [*Sov. Phys. Semiconductors* **22**, 630 (1988)].

¹²I. M. Tsidil'kovskii, G. I. Harus, and G. Shelushina, *Adv. Phys.* **34**, 43 (1985).

¹³G. L. Hansen, T. N. Schmit, and T. N. Gasselman, *J. Appl. Phys.* **53**, 7099 (1982).

¹⁴A. V. Germanenko, G. M. Min'kov, and O. E. Rut, *Poluprovodniki c Uzkoj Zapreshchenoi Zonnoi i Polumetalloy* (Narrow-Gap Semiconductors and Semimetals). Abstracts of the 7th All-Union Symposium, Part 1, Lvov, 1985, p. 100.

Translated by Frank J. Crowne